Geophysical Evidence that Saturn's Moon Phoebe Originated from a C-Type Asteroid Reservoir

Julie Castillo-Rogez, Pierre Vernazza, Kevin Walsh

Geophysical Evidence that Saturn's Moon Phoebe Originated from a C-Type Asteroid Reservoir

Julie Castillo-Rogez[1], Pierre Vernazza[2], Kevin Walsh[3]

(1) Jet Propulsion Laboratory, California Institute of Technology, Pasadena, CA, USA.

(2) Laboratoire d'Astrophysique de Marseille, UMR 7326 LAM, Aix-Marseille Universite, France.

(3) Southwest Research Institute, Boulder, CO, USA.

Abstract: Saturn's Moon Phoebe has been suggested to originate from the Kuiper Belt. However, its density is twice that of Kuiper Belt objects (KBOs) in the same size class, which challenges that relationship. Since the internal evolution of midsize planetesimals (100-300 km in diameter) is primarily driven by the amount of accreted short-lived radioisotopes, it is possible to constrain the relative times of formation of these bodies based on their bulk porosity content, hence their densities. From modeling the thermal evolution of KBOs, we infer a difference in formation timing between these bodies and Phoebe. This confirms prior suggestions for a delayed accretion timeframe with increasing distance from the Sun. This geophysical finding combined with spectral observations suggests Phoebe formed in the same region as C-type asteroids and support recent dynamical models for a C-type body reservoir between the orbits of the giant planets. On the other hand, the similarly low densities of midsize D-type asteroids, Trojan asteroids, and KBOs add to the growing evidence that these objects shared a common reservoir near or beyond the orbit of Neptune and were heat starved overall.

Keywords: Kuiper belt: general; Planetary Systems, planets and satellites: Interiors; Planetary Systems, minor planets, asteroids, general; Planetary Systems

1. Introduction:

The main belt of asteroids is composed of a variety of bodies. About half of the mass of the main belt is encompassed in the four most massive asteroids (Ceres, Vesta, Pallas, Hygiea). The rest of the main belt mass is dominated by mid-sized (100-300 km diameter) asteroids, which are

believed to be the source of the many fragments found in the belt (Bottke et al. 2005, Cuzzi et al. 2010) and the progenitors of asteroid families (Dermott et al. 2018). The current status quo is that these planetesimals accreted fast (Morbidelli et al. 2009) and thus represent the first generation of large bodies in the solar system (Bottke et al. 2005, Cuzzi et al. 2010). That class of bodies is a common feature of all the reservoirs of small bodies, although these objects are most frequently found in the main belt of asteroids and the Kuiper Belt. They are scarcer among the Jupiter Trojan asteroid clusters and irregular satellites (Fig. 1).

In water-rich mid-sized bodies, long-lived radioisotopes, which deliver their heat over billion-year timescales, have little bearing on internal evolution, especially since ice thermal conductivity is very high (5-16 W/m/K, Andersson and Inaba 2005) at the temperatures of interest. Furthermore, in their detailed review of small body heat sources, Leliwa-Kopystynski and Kossacki (2000) showed that accretional energy is a marginal heat source in bodies less than 500 km diameter. Hence, this leaves short-lived radioisotopes as the primary driver of thermal evolution in these objects. Their impact is a function of the relative fractions of rock and ice. The role of short-lived radioisotopes, and especially aluminum-26 (^{26}Al), in driving aqueous alteration in the parent bodies of carbonaceous chondrites was recognized early on (e.g., Schramm et al. 1970). In particular, the class of C*h* asteroids, most within 100-300 km, show evidence for aqueous alteration (Rivkin et al. 2015) and are believed to be parent bodies of the CM chondrites (e.g., Young et al. 1999, 2003; McAdam et al. 2015; Vernazza et al. 2016). Short-lived radioisotopes are also believed to have played a major role in the evolution of mid-sized Kuiper Belt objects (KBOs) and other transneptunian objects (TNOs) (e.g., Prialnik et al. 2008; Shchuko et al. 2014). However, the density data returned for representatives of these reservoirs over the past decade instead suggest they have preserved a large fraction of porosity, which is evidence for weakly evolved objects. On the other hand, Saturn's moon Phoebe, which was suggested to come from the Kuiper Belt (e.g., Johnson and Lunine 2005), has a density that is almost twice that of observed at KBOs.

We summarize the state of knowledge of 100-300 km planetesimals in Section 2. We use porosity as a gauge of internal evolution, following the approach of Castillo-Rogez et al. (2017), to compare the internal states of bodies formed with different amounts of (live) ^{26}Al. We focus on the modeling of KBO internal evolution for comparison with the Castillo-Rogez et al. (2012) modeling of Phoebe, as presented in Section 3. Since ^{26}Al has a short half-life (~0.71 My), the amount of ^{26}Al required to explain observed densities can been used as a chronometer, i.e., to constrain the time at which bodies fully assembled. Hence our results lead to new constraints on the relative formation timing of small bodies reservoirs found across the solar system and their genetic relationships, as discussed in Section 4.

2. Overview of Planetesimal Densities

Hydrated C-type asteroids (C*h* and C*gh*-types) have densities in the 1.4-2.5 g/cm^3 range [e.g., Hanus et al. 2017] with a marked dependence on size, as previously noted by Carry (2012). That

density range may reflect a low fraction of free volatiles (ice) combined with a low porosity fraction, especially at increasing sizes. Densities between 1.6-2.2 g/cm^3 obtained for bodies 100-200 km in diameter matches their meteoritic analogs, namely CM chondrites (average density ~2.1 g/cm^3, Consolmagno et al. 2008). Times of formation for these bodies believed to be parent bodies of CM chondrites (Vernazza et al. 2016) is 3.5 My after CAIs (Jogo et al. 2017) assuming a canonical $^{26}Al/^{27}Al = 5.5x10^{-5}$. Densities of IDP-like C-type asteroids (these objects represent ~50% of C-complex asteroids and possess spectral properties unlike those of CM chondrites; Vernazza et al. 2015, 2017) show a large spread, beyond the large uncertainties, with densities ranging between 1.0-1.6 g/cm^3 for bodies in the 100-200 km size range.

Many irregular satellites share several similarities with C-asteroids. This is the case of Saturn's irregular satellite Phoebe, high-density body (1.67 g/cm^3, Thomas et al. 2007). Outer solar system bodies in the same size range for which density data are available (besides icy moons) show much lower densities (Figure 1). Phoebe also displays expressions of aqueous alteration and geophysical evolution explained by an early phase of melting driven by ^{26}Al decay heat (Castillo-Rogez et al. 2012) and an ice-rich subsurface (below the regolith) (Clark et al. 2005; Fraser and Brown 2018). The density of another irregular satellite, Jupiter's moon Himalia was inferred to be also about 1.63 g/cm^3, assuming a mean radius of ~85 km (Cruikshank 1977), and even larger for the lower bound on radius determination of ~65 km (Porco et al. 2003). Detailed analysis of Himalia's impact on the orbits of neighboring satellites by Brozovic and Jacobson (2017) yields a similar density, between 1.55 and 2.26 g/cm^3.

On the other hand, Kuiper Belt objects smaller than 500 km in diameter have densities around 0.6 g/cm^3 and down to 0.3 g/cm^3 whereas those objects bigger than 800 km have densities >1 g/cm^3 (Stansberry et al. 2012; Brown 2013). Above 500 km diameter, KBOs show a quasi-linear density dependence on size, up to 2.5 g/cm^3 (Brown 2013). Brown (2013) pointed out that the density of 0.82±0.11 g/cm^3 he inferred for the 650-km large 2002UX25 reflects both substantial porosity and a deficit in rock. Larger KBOs have densities that do reflect a rock-rich interior. This diversity has been interpreted by Barr and Schwamb (2016) as evidence for the partial removal of ice shells from differentiated KBOs. Hence rock scarcity cannot uniquely account for the large porosity preserved in midsize KBOs.

P- and D-type asteroids found in the main belt have relatively low densities: ~1 g/cm^3 for the large (250 km) 65 Cybele and its family members: e.g., 87 Sylvia (1.2±0.15 g/cm^3, Marchis et al. 2012). Furthermore, large D- and P-types do not show evidence for hydration, similarly to Trojan asteroids. The ~270 km P-type 65 Cybele's surface displays water ice (Licandro et al. 2011). Few density measurements have been obtained for Trojan asteroids: $0.8^{+0.2}_{/-0.1}$ g/cm^3 for Patroclus (Marchis et al. 2006) and 1±0.2 g/cm^3 for Hektor (Marchis et al. 2014), although a much higher estimate of 2.43±0.35 g/cm^3 has been suggested for the latter (Descamps 2015). Marchis et al. (2014) pointed out that the difference between the densities of Patroclus and Hektor is consistent with the difference in compaction driven by the pressures that can be reached in these objects, assuming that they started with similar, volatile-rich compositions.

Density measurements are lacking for Centaurs, but indirect observations also suggest these objects have low densities. For example, an upper bound density of 0.9 g/cm^3 was derived for the ~200-km large Chiron (Meech et al. 1997) and the ~190 km Pholus has a density of the order of 0.5 g/cm^3 (Tegler et al. 2004). A large transneptunian objects, the 920-km large Orcus has a density of $1.53^{+0.15}_{-0.13}$ g/cm^3 (Fornasier et al. 2014). It displays potential spectral evidence for ammonium (Delsanti et al. 2010), a marker of aqueous alteration like in the case of Ceres (De Sanctis et al. 2015), although other types of nitrogen compounds can explain the Orcus spectra (e.g., NH_3, Delsanti et al. 2010).

These discrepancies show that midsize planetesimals across the solar system underwent different evolutionary pathways where composition alone cannot account for the disparities in densities.

3. Results: Internal Evolution of Objects Formed in the Transneptunian Region

We model porosity evolution and the possible occurrence of aqueous alteration in several examples of midsized bodies representing Phoebe-like bodies formed with various amounts of ^{26}Al. The approach is similar to Castillo-Rogez et al. (2007, 2012, 2017) and Marchis et al. (2014) using porosity evolution data for various icy compositions (e.g., Leliwa-Kopystynski and Kossacki 2000; Durham et al. 2005) and accounting for the insulating effect (i.e., lower thermal conductivity) of porosity (Shoshany et al. 2002). We assume accretion is near instantaneous (Leliwa-Kopystynski and Kossacki 2000). It has generally been assumed that the relative fractions of ice and rock for objects formed in the solar nebula was determined by nebula temperatures and the form (reduced or oxidized) taken by carbon, with grain densities ranging from about 1.5 to 2.2 g/cm^3 (Wong et al. 2008; Castillo-Rogez et al. 2012). We use 1.5 g/cm^3 and 1.8 g/cm^3 as references densities for this modeling since the resulting models yields the best fits to the observations. The corresponding mass fractions of dry rock ranges from about 53% to 67%. We also assume a starting bulk porosity of 50% in all our models. While icy bodies in the far outer Solar system contain second-phase impurities that can promote low temperature compaction creep, their abundances are not constrained. Here, we assume that relaxation is only driven by ice. This endmember case yields a bound on the amount of compaction driven by thermal evolution. We track microporosity evolution but not macroporosity introduced by impacts or subcatastrophic collision and reaccretion that may contribute 10-15% of the overall porosity. Lastly, we account for the impact of aqueous alteration on material thermophysical properties, following the approach presented in Castillo-Rogez et al. (2019).

Results are presented in Figure 2. Short-lived radioisotopes represent a powerful heat source that can drive long-term geophysical evolution. Times of formation of 3 and 3.5 My after CAIs allows early ice melting, aqueous alteration, and separation of an ice rich shell (Fig. 2a and 2b). In these examples, compaction and most of the thermal evolution occurs during the first 10s My after formation and the body freezes by 100 My. The impact of long-lived radioisotopes is negligible because of the high thermal conductivity of ice at 30 K (~16 W/m/K, Andersson and Inaba 2005).

The most recent estimate for the lifetime of the solar nebula based on magnetic measurements of meteorites is about 4 My (Wang et al. 2017). Weaker ^{26}Al decay heat resulting from later times of formation leads to partial compaction for 4 My after CAIs (Fig. 2c) or insignificant compaction if the time of formation is longer than ~4.5 My after CAIs (Figs 2e, f). Hence, just 1 My delay in the formation of a Phoebe-like body leads to a very different outcome. If Phoebe-sized TNOs accreted after 4 My, then a slightly lower density (e.g., 1500 kg/m3, Fig. 2d), greater initial porosity, and/or significant macroporosity are needed to reproduce a density of <1 g/cm^3 generally observed in that group of bodies (Fig. 1). Another example, for a body 250 km in radius also suggests a grain density lower than that required for Phoebe (Figure 3). A density of 1500 kg/m^3 yields a bulk density of ~1300 kg/m^3, which appears consistent with observations (noting the small sample) (Fig. 3b).

For TNOs greater than 250 km in radius, the linear trend in the density versus size seen in Figure 1 can be ascribed to the combined effect of size and long-lived radioisotope decay heat. Macroporosity could shift the bulk density toward lower values, while material loss from impacts at differentiated bodies and redistribution of volatiles upon heating could increase it (Barr and Schwamb 2016). A more detailed study is required to narrow down the original grain density of KBOs.

In summary, the preservation of >50% porosity in certain classes of small bodies can be directly ascribed to a scarcity in short-lived radioisotopes. The contrast in formation temperatures between these reservoirs is not sufficient to explain the difference in evolution. These results suggest that interior evolution of midsized KBOs was more limited than previously anticipated (e.g., Merk and Prialnik 2006; Desch et al. 2009). Similar evolution between Trojan asteroids, P- and D-type asteroids found in the main belt, Centaurs, and KBOs support a genetic relationship between these classes of bodies, as simulated by many studies (Morbidelli et al. 2005; Wong and Brown 2015, Levison et al. 2009; Vernazza et al. 2015, Vernazza and Beck 2017). This also suggests that P and D type asteroids found throughout the Solar system were barely chemically evolved and offer truly pristine material to sample below their weathered crust.

4. Discussion and Conclusions:

Phoebe was suggested to come from the Kuiper Belt based on the observation that its density matches the grain density inferred from cosmochemical models (Johnson and Lunine 2005; Castillo-Rogez et al. 2012). The density contrast between Phoebe and KBO questions that relationship. Thermal modeling confirms earlier work showing that most of Phoebe's original porosity could be removed provided that it accreted in ~3-3.5 My My after calcium-aluminum inclusions (Castillo-Rogez et al. 2012). Furthermore, Phoebe displays hydrated material on its surface, which is consistent with internal evolution involving aqueous alteration simulated for times of formation of 3-3.5 My after CAIs (Fig. 2a.b). Himalia and most of its family members display a flat spectrum in the 0.4-0.9 μm range and similar spectral properties in the visible and near infra-red as certain C-type asteroids, for example 52 Europa (Brown and Rhoden 2014; Bhatt et al. 2017). Phoebe and Himalia contrast with other irregular satellites showing a reddening that might link them to the classes of P and D asteroids (e.g., Themisto, Ananke). The

latter have been interpreted as evidence for an origin of irregular satellites from a reservoir shared with KBOs. On the other hand, the similarities between the spectra of Phoebe, Himalia, and C-type asteroids was interpreted as evidence that the two irregular satellites actually migrated from the main belt of asteroids (e.g., Hartmann 1987). As an alternative, early giant planet migration and/or planetary growth (Walsh et al. 2011; Raymond and Izidoro 2017; Ronnet et al. 2018) could provide a scenario for a common origin for hydrated C-type asteroids and some irregular satellites from between the orbits of the giant planets. This model implies accretion was early and fast in that region, consistent with recent accretion scenarios (e.g., Johansen et al. 2015). As a corollary, this model suggests bodies in the Jupiter-Uranus region formed fast enough for ^{26}Al to play a role in their geophysical evolution, as suggested for Iapetus (Castillo-Rogez et al. 2007). On the other hand, short-period comets, if they are connected to the Kuiper Belt, also formed with little or no ^{26}Al, contrary to previous assumptions (e.g., Gounelle et al. 2008). The long required time of formation for TNOs, potentially longer than 4 My needs to be reconciled with the current estimate for the solar nebula lifetime (Wang et al. 2017). Certain processes, such as the latent heat of supervolatile ice vaporization, need to be accounted for in order to derive a most accurate timeline of events in the outer solar system.

New main belt asteroid densities are necessary to assess whether the scattering observed across that class of bodies in Figure 1 is real and can potentially reflect different origins across the solar system for the various types of C-type asteroids. Density constraints will become available from observations with the Very Large Telescope at mid-sized main belt asteroids in the 2019-2020 timeframe (HARISSA Project, Vernazza et al. 2018) and by the Lucy mission at the Jupiter Trojans.

Lastly, Phoebe's evolved interior needs to be reconciled with the very high D/H ratio (0.0013±0.0003) recently inferred from the infrared observations returned by the Cassini mission (Clark et al., 2019). This high value is an order of magnitude higher than that of Jupiter-Family-Comets and its meaning remains to be further understood, especially if Phoebe is not a pristine object.

Acknowledgements: The authors are grateful to Sean Raymond for his comments, which significantly improved the quality of this manuscript. JCCR is thankful to Hap McSween, Driss Takir, and Orkan Umurhan for feedback. Part of this work was carried out at the Jet Propulsion Laboratory, California Institute of Technology, under contract to NASA. Government sponsorship acknowledged.

Reference List:

Andersson, O, Inaba, A (2005) Thermal conductivity of crystalline and amorphous ices and its implications on amorphization and glassy water, Physical Chemistry Chemical Physics 7, 1441-1449.

Baer, J., Chesley, S. R., Matson, R. D. (2011) Astrometric masses of 26 asteroids and observations on asteroid porosity, Astron. J. 141:143 (12pp)

Baer, J., Chesley, S. R. (2008) Astrometric masses of 21 asteroids, and an integrated asteroid ephemeris, Celestial Mech Dyn Astr (2008) 100:27–42.

Barr, Amy C., Schwamb, Megan E. (2016) Interpreting the densities of the Kuiper belt's dwarf planets, *Monthly Notices of the Royal Astronomical* Society 460, 1542-1548

Bhatt, M., Reddy, V., Schindler, K., Cloutis, E., Bhardwaj, A., Corre, L. L., Mann, P. (2017) Composition of Jupiter irregular satellites sheds light on their origin, Astronomy and Astrophysics 608, A67.

Bottke, W., Jr., Durda, D. D., Nesvorny, D., Jedicke, R., Morbidelli, A., Vokrouhlicky, D., Levison, H. (2005) The fossilized size distribution of the main asteroid belt, *Icarus* 175, 111-140.

Brown, M. E. (2013) The Density of Mid-sized Kuiper Belt Object 2002 UX25 and the Formation of the Dwarf Planets, The Astrophysical Journal Letters 778, id. L34.

Brown, M. E., Rhoden, A. R. (2014) The 3 μm spectrum of Jupiter's irregular satellite Himalia, Astroph. J. Lett. 793, L44.

Castillo-Rogez J., D. L. Matson, C. Sotin, T. V. Johnson, J. I. Lunine, P. C. Thomas (2007) Iapetus' Geophysics: Rotation Rate, Shape, and Equatorial Ridge, *Icarus*, doi:10.1016/j.icarus.2007.02.018.

Castillo-Rogez, J., Johnson, T., Thomas, P., Choukroun, M., Matson, D., Lunine, J. (2012) Evolution of Phoebe, a large planetesimal in the outer Solar system, *Icarus* 219, 86-109.

Castillo-Rogez, J. C., Walsh, K. J., Vernazza, P., Takir, D. (2017) Constraints on the time of formation of Ceres and Ceres-like asteroids – A joint reservoir with C-type irregular satellites?

Clark, R. N., Brown, R. H., Jaumann, R., Cruikshank, D. P., Nelson, R. M., et al. (2005) Compositional maps of Saturn's moon Phoebe from imaging spectroscopy, Nature 435, 66-69.

Clark, R. N., Brown, R. H., Cruikshank, D. P., Swayze, G. (2019) Isotopic Ratios of Saturn's Rings and Satellites: Implications for the Origin of Water and Phoebe, Icarus in press, https://doi.org/10.1016/j.icarus.2018.11.029

Consolmagno, G., D. Britt, R. Macke. The significance of meteorite density and porosity. Chemie der Erde – *Geochemistry* 68, 1-29, 2008.

Cruikshank, D. P. (1977) Radii and albedos of four Trojan asteroids and Jovian satellites 6 and 7, Icarus 30, 224.

Cuzzi, J. N., Hogan, R. C., Bottke, W. B. (2010) Towards initial mass functions for asteroids and Kuiper Belt Objects, *Icarus* 208, 518-538.

Delsanti, A., Merlin, F., Guilbert-Lepoutre, A., Bauer, J., Yang, B., Meech, K. J. (2010) Methane, ammonia, and their irradiation products at the surface of an intermediate-size KBO? A portrait of Plutino (90482) Orcus, Astronomy and Astrophysics 520, id. A40.

Dermott, S. F., Christou, A. A., Li, D., Kehoe, T. J. J., Robinson, J. M. (2018) The common origin of family and non-family asteroids, Nature Astronomy 2, 549-554.

De Sanctis, M. C., E. Ammannito, A. Raponi, S. Marchi, T. B. McCord, H. Y. McSween, F. Capaccioni et al. (2015) Ammoniated phyllosilicates with a likely outer Solar System origin on (1) Ceres, *Nature* 528, 241-244.

Descamps, P. (2015) Dumb-bell-shaped equilibrium figures for fiducial contact-binary asteroids and EKBOs, Icarus 245, 64-79.

Desch, Steven J., Cook, Jason C., Doggett, T. C., Porter, Simon B. (2009) Thermal evolution of Kuiper belt objects, with implications for cryovolcanism, *Icarus* 202, 694-714.

Durda, D. D., Bottke, W. F., Nesvorny, D., Enke, B. L., Merlin, W. J., Asphaug, E., Richardson, D. C. (2007) Size–frequency distributions of fragments from SPH/*N*-body simulations of asteroid impacts: Comparison with observed asteroid families, *Icarus* 186, 498-516.

Durham, W. B., McKinnon, W. B., Stern, L. A. (2005) Cold compaction of water ice, Geophys. Res. Lett. 32, L18202.

Fornasier, S., Lantz, C., Barucci, M. A., Lazzarin, M. (2014) Aqueous alteration on main belt primitive asteroids: Results from visible spectroscopy, *Icarus* 233, 163-178.

Fraser, W. C., Brown, M. E. (2018) Phoebe: A Surface Dominated by Water, *The Astronomical Journal* 156, 13 pp.

Goffin, E. (2014) Astrometric asteroid masses: a simultaneous determination, Astronomy and Astrophysics 565, A56.

Guilbert-Lepoutre, A. (2011) A thermal evolution model of Centaur 10199 Chariklo, *Astron. J.* 141, 103.

Guilbert, A., Barucci, M. A., Brunetto, R., Delsanti, A., Merlin, F., Alvarez-Candal, A., Fornasier, S., de Bergh, C., Sarid, G. (2009) A portrait of Centaur 10199 Chariklo, *Astron & Astroph.* 501, 777-784.

Hartmann, W. K. (1987) A satellite-asteroid mystery and a possible early flux of scattered C-class asteroids, Icarus 71, 57-68.

Hanuš, J., Marchis, F., Durech, J. (2013) Sizes of main-belt asteroids by combining shape models and Keck adaptive optics observations, Icarus 246, 1045-1057.

Hanuš, J., Viikinkoski, M., Marchis, F., Ďurech, J., Kaasalainen, M., Delbo', M., Herald, D., Frappa, E., Hayamizu, T., Kerr, S., Preston, S., Timerson, B., Dunham, D., Talbot, J. (2017) Volumes and bulk densities of forty asteroids from ADAM shape modeling, Astron. Astroph. 601, id.A114, 41 pp.

Johansen, A., Mac Low, M.-M., Lacerda, P., Bizzarro, M. (2015) Growth of asteroids, planetary embryos, and Kuiper belt objects by chondrule accretion, Science Advances 2015;1:e1500109.

Jogo, K., Nakamura, T., Ito, M., Wakita, S., Zolotov, M. Y., Messenger, S. R. (2017) Mn-Cr ages and formation conditions of fayalite in CV3 carbonaceous chondrites: Constraints on the accretion ages of chondritic asteroids, *Geochimica and Cosmochimica Acta* 199, 58-74.

Johnson, Torrence V., Lunine, Jonathan I. (2005) Saturn's moon Phoebe as a captured body from the outer Solar System, Nature 435, 69-71.

Kenyon, S. J., Bromley, B. C., O'Brien, D. P., Davis, D. R. (2008) Formation and collisional evolution of Kuiper Belt objects, In: The Solar System Beyond Neptune, Ed. A. Barucci, 293-312.

Leliwa-Kopystynski, J., Kossacki, K. J. (2000) Evolution of porosity in small icy bodies, Planetary and Space Science 48, 727-745.

Levison, H. F., Bottke, W. F., Gounelle, M., Morbidelli, A., Nesvorný, D., Tsiganis, K. (2009) Contamination of the asteroid belt by primordial trans-Neptunian objects, Nature 460, 364-366.

Licandro, J., Campins, H., Kelley, M., Hargrove, K., Pinilla-Alonso, N., Cruikshank, D., Rivkin, A. S., Emery, J. (2011) (65) Cybele: detection of small silicate grains, water-ice, and organics, Astronomy and Astrophysics 525, id. A34.

Marchis, F., Kaasalainen, M., Hom, E. F. Y., Berthier, J., Enriquez, J., Hestroffer, D., Le Mignant, D., de Pater, I. (2006) Shape, size and multiplicity of main-belt asteroids. I. Keck Adaptive Optics survey, Icarus 185, 39-63.

Marchis, F. Enriquez, J. E., Emery, J. P., Mueller, M., Baek, M., Pollock, J., Assafin, M., Vieira Martins, R., Berthier, J., Vachier, F., Cruikshank, D. P., Lim, L. F., Reichart, D. E., Ivarsen, K. M., Haislip, J. B., LaCluyze, A. P. (2012) Multiple asteroid systems: Dimensions and thermal properties from Spitzer Space Telescope and ground-based observations, Icarus 221, 1130-1161.

Marchis, F., Vachier, F., Durech, J., Enriquez, J. E., et al. (2013) Characteristics and large bulk density of the C-type main-belt triple asteroid (93) Minerva, Icarus 224, 178-191.

Marchis, F., Durech, J., Castillo-Rogez, J., Vachier, F., Cuk, M., Berthier, J., Wong, M. H., Kalas, P., Duchene, G., van Dam, M. A., Hamanowa, H., Viikinkoski, M. (2014) The Puzzling Mutual Orbit of the Binary Trojan Asteroid (624) Hektor, The Astrophysical Journal Letters 783, id. L37.

McAdam M. M., Sunshine J. M., Howard K. T. and McCoy T. J., 2015. Aqueous alteration on asteroids: Linking the mineralogy and spectroscopy of CM and CI chondrites, *Icarus* 245, 320-332.

Meech, K. J., Buie, M. W., Samarasinha, N. H., Mueller, B. E. A., Belton, M. J. S. (1997) Observations of Structures in the Inner Coma of Chiron with the HST Planetary Camera, Astronomical Journal 113, 844-862.

Merk, R., Prialnik, D. (2006) Combined modeling of thermal evolution and accretion of trans-neptunian objects – Occurrence of high temperatures and liquid water, Icarus 183, 283-295.

Morbidelli, A., Levison, H. F., Tsiganis, K., Gomes, R. (2005) Chaotic capture of Jupiter's Trojan asteroids in the early Solar System, Nature 435, 462-465.

Morbidelli, A., Bottke, W. F., Nesvorny, D., Levison, H. F. (2009) Asteroids were born big, *Icarus* 204, 558-573.

Pajuelo, M., Carry, B., Vachier, F., Marsset, M., Berthier, J., Descamps, P., Merline, W. J., Tamblyn, P. M., Grice, J., Conrad, A., Storrs, A., Timerson, B., Dunham, D., Preston, S., Vigan, A., Yang, B., Vernazza, P., Fauvaud, S., Bernasconi, L., Romeuf, D., Behrend, R., Dumas, C., Drummond, J. D., Margot, J.-L., Kervella, P., Marchis, F., Girard, J. H. (2018) Physical, spectral, and dynamical properties of asteroid (107) Camilla and its satellites, Icarus 309, p. 134-161.

Porco, C. C., et al. (2003) Cassini imaging of Jupiter's atmosphere, satellites, and rings, Science 299, 1541-1547.

Prialnik, D., Sarid, G., Rosenberg, E. D., Merk, R. (2008) Thermal and chemical evolution of comet nuclei and Kuiper Belt objects, Space Science Reviews 138, 147-164.

Rivkin, A. S., Thomas, C. A., Howell, E. S., Emery, J. P. (2015) The Ch-class Asteroids: Connecting a Visible Taxonomic Class to a 3 μm Band Shape, Astron. J. 150, id 198.

Ronnet, T., O. Mousis, P. Vernazza, J. Lunine, A. Crida. Saturn's Formation and Early Evolution at the Origin of Jupiter's Massive Moons. AJ 155, 2018.

Schramm, D. N., Tera, F., Wasserburg, G. J. (1970) The isotopic abundance of ^{26}Mg and limits on ^{26}Al in the early solar system, Earth and Planetary Science Letters 10, 44-59.

Shschuko, O. B., Shschuko, S. D., Kartashov, D. V., Orosei, R. (2014) Conditions for liquid or icy core existence in KBO objects: Numerical simulations for Orcus and Quaoar, Planetary and Space Science 104 Part A, 147-155.

Shoshany, Y., Prialnik, D., Podolak, M. (2002) Monte Carlo Modeling of the Thermal Conductivity of Porous Cometary Ice, Icarus 157, 219-227.

Stansberry, J. A., Grundy, W. M., Mueller, M., Benecchi, S. D., Rieke, G. H., Noll, K. S., Buie, M. W., Levison, H. F., Porter, S. B., Roe, H. G. (2012) Physical properties of trans-neptunian binaries (120347) Salacia-Actaea and (42355) Typhon-Echidna, Icarus 219, 676-688.

Stern, S. A., et al. (2015) The Pluto system: Initial results from its exploration by New Horizons, Science 350, 249–352.

Takato, N., Bus, S. J., Terada, H., Pyo, T.-S., Kobayashi, N. (2004) Detection of a Deep 3-μm Absorption Feature in the Spectrum of Amalthea (JV), Science 306, 2224-2227.

Tegler, S. C., Romanishin, W., Consolmagno, G. J., Rall, J., Worhatch, R., Nelson, M., Weidenschilling, S. (2005) The period of rotation, shape, density, and homogeneous surface color of the Centaur 5145 Pholus, Icarus175, 390-396.

Thomas, P. C., Burns, J. A., Helfenstein, P., Squyres, S., Veverka, J., Porco, C., Turtle, E. P., McEwen, A., Denk, T., Giese, B., Roatsch, T., Johnson, T. V., Jacobson, R. A. (2007) Shapes of the saturnian icy satellites and their significance, Icarus 190, 573-584.

Vernazza, P., Marsset, M., Beck, P., Binzel, R. P., Birlan, M., Cloutis, E. A., DeMeo, F. E., Dumas, C., Hiroi, T. (2016) Compositional homogeneity of CM parent bodies, Astron. J. 152, 54 (10pp).

Vernazza, P., M. Marsset, P. Beck, R. P. Binzel, M. Birlan, R. Brunetto, F. E. DeMeo, Z. Djouadi, C. Dumas, S. Merouane, O. Mousis, B. Zanda. Interplanetary Dust Particles as Samples of Icy Asteroids. The Astrophysical Journal 806, 10p. (2015).

Vernazza, P., J. Castillo-Rogez, P. Beck et al. Different origins or different evolutions? Decoding the spectral diversity among C-type asteroids. Astron. J. 153, 2017.

Vernazza, P., P. Beck. Composition of Solar System Small Bodies. In Planetesimals: Early Differentiation and Consequences for Planets (L. T. Elkins-Tanton, B. P. Weiss, eds.), Cambridge University Press, 2017.

Vernazza, P., Brož, M., Drouard, A., Hanuš, J., Viikinkoski, M., Marsset, M., Jorda, L., Fetick, R., Carry, B., Marchis, F., Birlan, M., Fusco, T., Santana-Ros, T., Podlewska-Gaca, E., Jehin, E., Ferrais, M., Bartczak, P., Dudziński, G., Berthier, J., Castillo-Rogez, J., Cipriani, F., Colas, F., Dumas, C., Ďurech, J., Kaasalainen, M., Kryszczynska, A., Lamy, P., Le Coroller, H., Marciniak, A., Michalowski, T., Michel, P., Pajuelo, M., Tanga, P., Vachier, F., Vigan, A., Warner, B., Witasse, O., Yang, B., Asphaug, E., Richardson, D. C., Ševeček, P., Gillon, M., Benkhaldoun, Z. (2018) The impact crater at the origin of the Julia family detected with VLT/SPHERE? Astronomy & Astrophysics 618, id.A154, 16 pp.

Vilenius, E., Kiss, C., Mommert, M., Müller, T., Santos-Sanz, P., Pal, A., Stansberry, J., Mueller, M., Peixinho, N., Fornasier, S., Lellouch, E., Delsanti, A., Thirouin, A., Ortiz, J. L., Duffard, R., Perna, D., Szalai, N., Protopapa, S., Henry, F., Hestroffer, D., Rengel, M., Dotto, E., Hartogh, P. (2012) TNOs are Cool": A survey of the trans-Neptunian region. VI. Herschel/PACS observations and thermal modeling of 19 classical Kuiper belt objects, Astronomy & Astrophysics 541, id.A94, 17 pp.

Walsh, Kevin J., Morbidelli, A., Raymond, S. N., O'Brien, D. P., Mandell, A. M. (2011) A low-mass for Mars from Jupiter's early gas-driven migration, Nature 475, 206-209.

Wang, H., Weiss, B. P., Bai, X.-N., Downey, B. G., Wang, J., Wang, J., Suavet, C., Fu, R. R., Zucolotto, M. E. (2017) Lifetime of the solar nebula constrained by meteorite paleomagnetism, Science 355, 623-627, doi: 10.1126/science.aaf5043.

Yeomans, D. K., Barriot, J.-P., Dunham, D. W., Farquhar, R. W., Giorgini, J. D., Helfrich, C. E., Konopliv, A. S., McAdams, J. V., Miller, J. K., Owen, W. M., Jr., Scheeres, D. J., Synnott, S. P., Williams, B. G. (1997) Estimating the Mass of Asteroid 253 Mathilde from Tracking Data During the NEAR Flyby, Science 278, 2106, doi:10.1126/science.278.5346.2106

Young E. D., Ash R. D., England P., Rumble D., III (1999) Fluid flow in chondrite parent bodies: deciphering the compositions of planetesimals, *Science* 286, 1331-1335.

Young E. D., Zhang K. K. and Schubert G. (2003) Conditions for pore water convection within carbonaceous chondrite parent bodies - implications for planetesimal size and heat production, *Earth and Planetary Science Letters*, 213, 249-259.

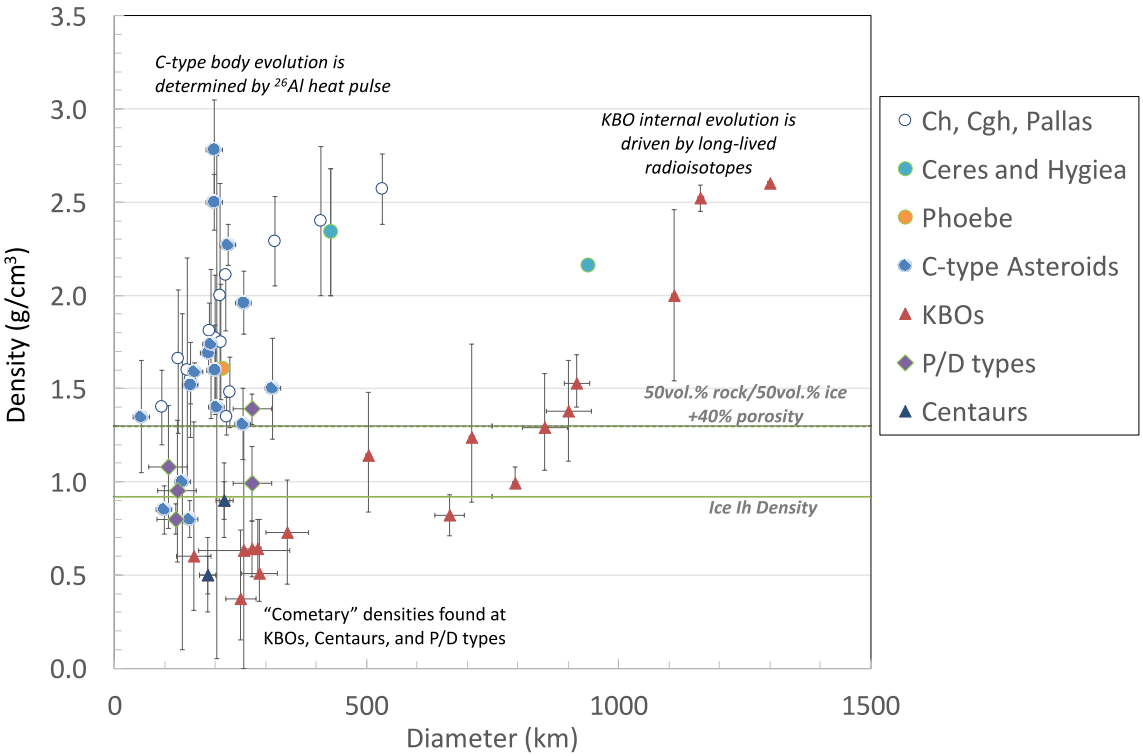

Figure 1. Bulk densities of minor planets less than 1500 km in diameter. Ice I density (solid line) and a mixture of 50vol.% rock/50vol.% ice with 40% porosity added (dashed line) are shown for reference. The spread in the 100-300 km region illustrates the contrast in remnant porosity and thus heat budget available to these various classes of bodies. Two clusters of bodies can be distinguished with densities <~1g/cm^3 and >~1.3 g/cm^3. Additional data for large (>1000km) KBOs is provided to support the discussion. References for asteroids: Yeomans et al. (1997), Mueller et al. (2009), Fienga et al. (2010), Marchis et al. (2006, 2008, 2012, 2013), Baer and Chesley (2008), Baer et al. (2011), Goffin (2014), Hanus et al. (2016), Hanus (2017), Pajuelo et al. (2018). References for TNOs: Meech et al. (1997), Tegler et al. (2004), Grundy et al. (2012), Vilenius et al. (2012), Brown (2013), Marchis et al. (2014).

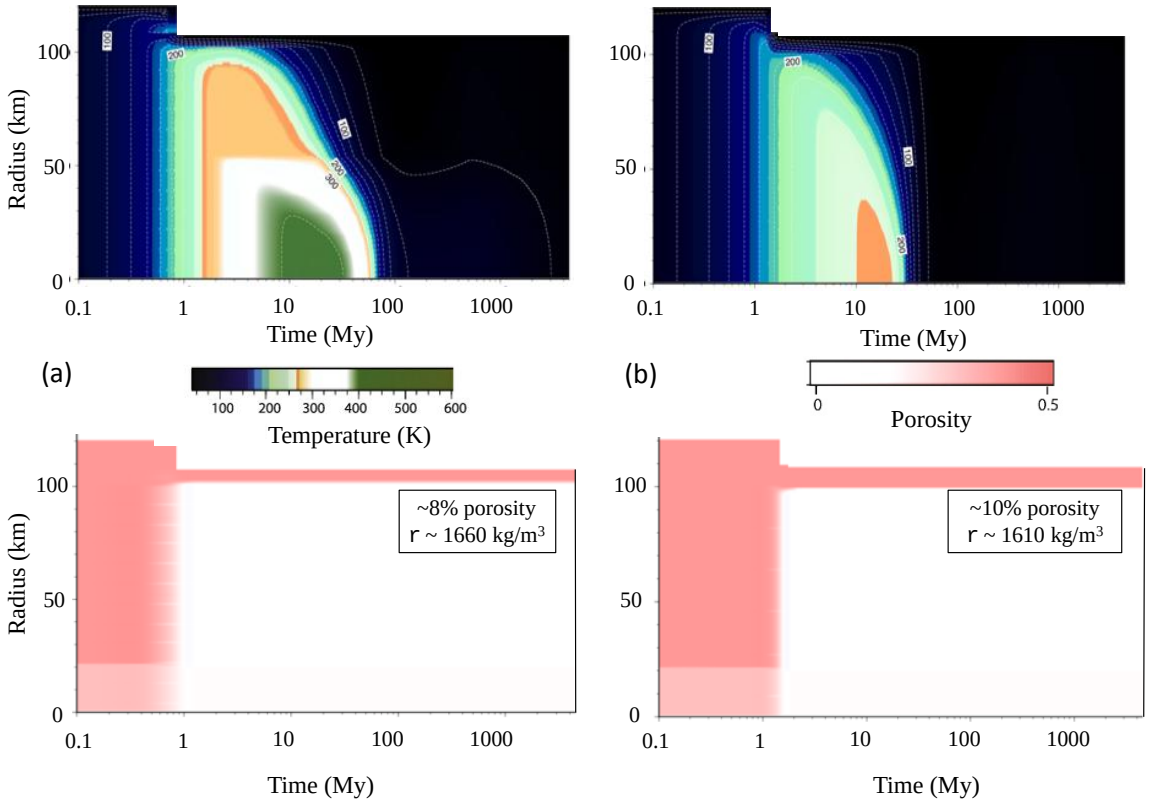

Figures 2a, b. Thermal and porosity evolution of Phoebe (~107 km radius) assuming a time of formation of (a) 3 My and (b) 3.5 My after CAIs, a grain density of 1.8 g/cm^3, an initial bulk porosity of 50%, and a formation temperature of 30 K. The final porosity and bulk density are indicated in the boxes.In these two cases, the final bulk density is close to the observed density of 1.63 g/cm^3.

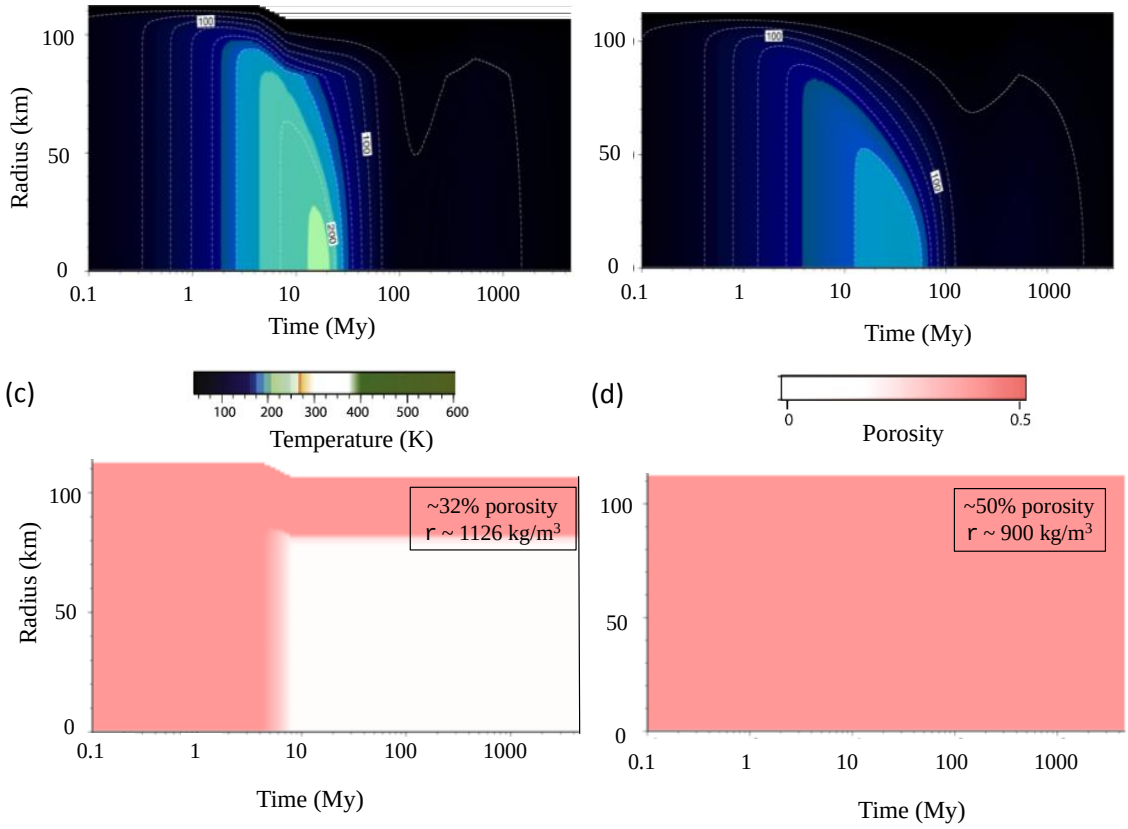

Figures 2c, d. Same as 2a but assuming a Phoebe-like body formed in the transneptunian region, a time of formation of 4 My after CAIs, and a gain density of (c) 1800 kg/m^3 and (d) 1500 kg/m^3.

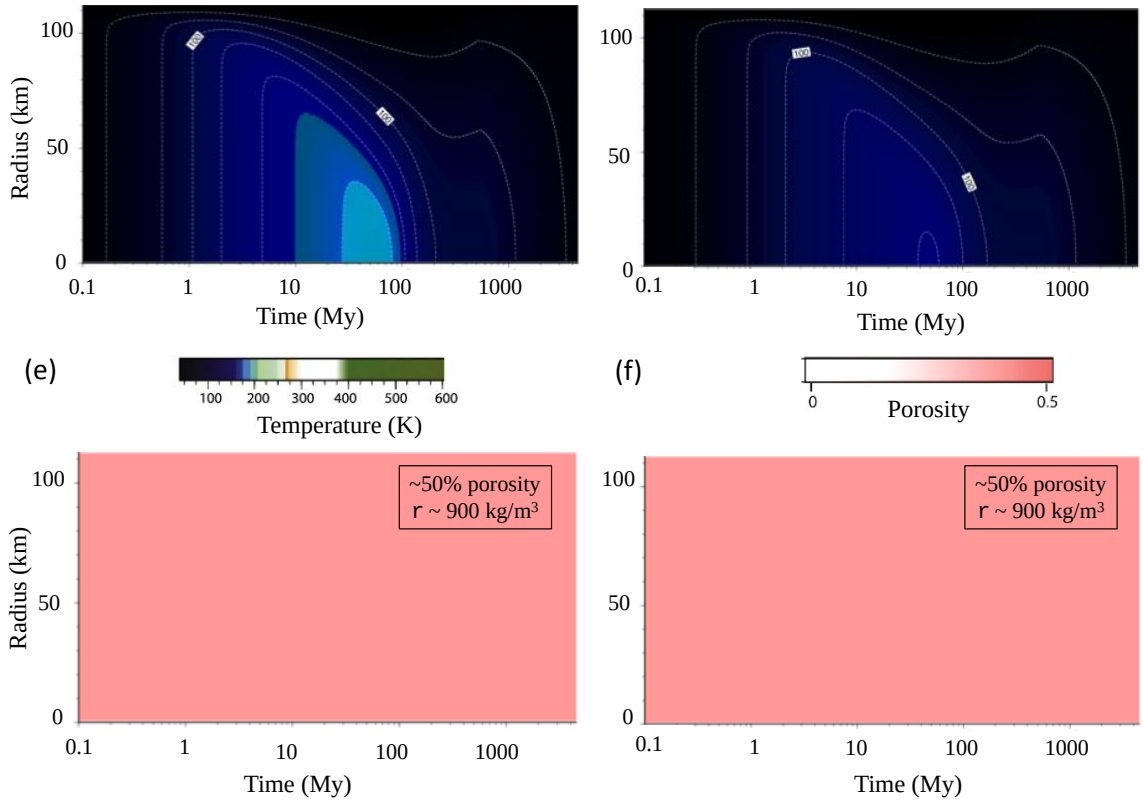

Figures 2e, f. Same as 2a (grain density of 1800 kg/m^3) for times of formation of (e) 4.5 My and (f) 5 My after CAIs.

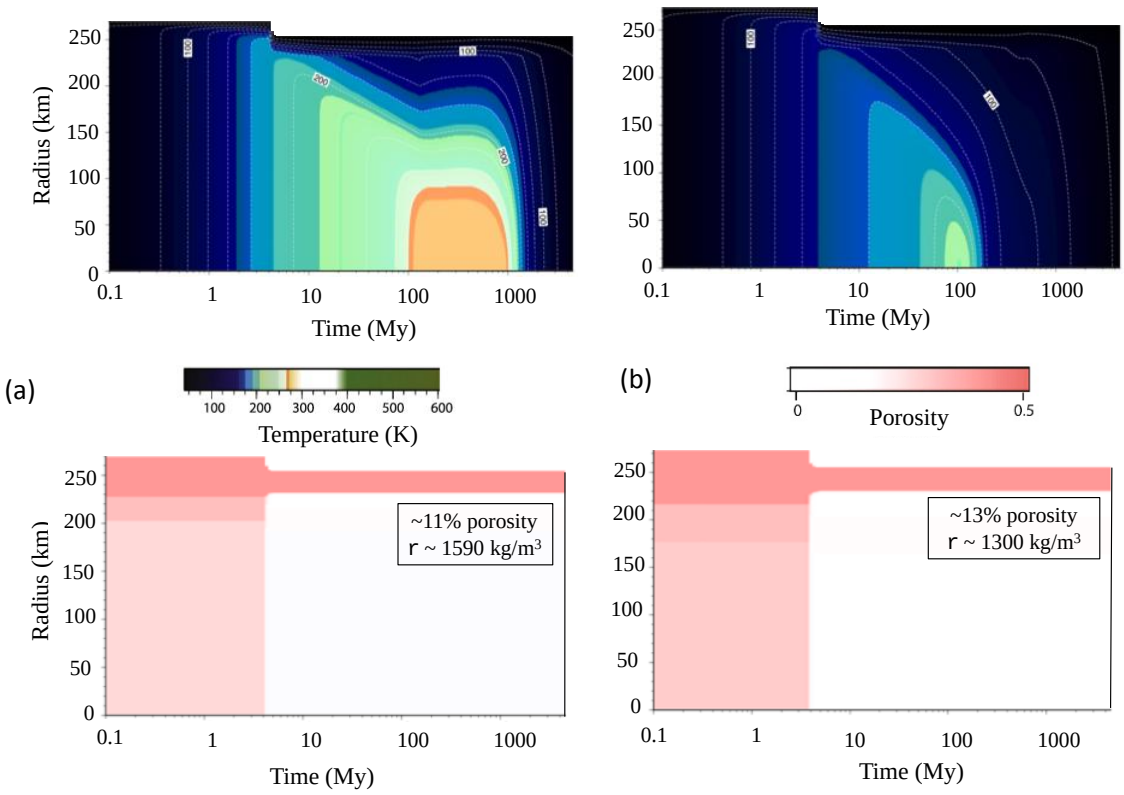

Figure 3. Same as Figure 2, but for a 250-km radius object, a time of formation of 4 My after CAIs, and a grain density of (a) 1800 kg/m^3) and (b) 1500 kg/m^3.